Pharmaceutical Research, Vol. 25, No. 8, August 2008 (© 2008)
DOI: 10.1007/s11095-008-9611-6

Research Paper

In Vitro and *In Vivo* Investigation on PLA–TPGS Nanoparticles for Controlled and Sustained Small Molecule Chemotherapy

Zhiping Zhang,[1,4] Sie Huey Lee,[2,5] Chee Wee Gan,[1] and Si-Shen Feng[1,2,3]

Received January 16, 2008; accepted April 25, 2008; published online May 29, 2008

Purpose. The aim of this work was to evaluate *in vivo* poly(lactide)-D-α-tocopheryl polyethylene glycol 1,000 succinate nanoparticles (PLA–TPGS NPs) for controlled and sustained small molecule drug chemotherapy.
Methods. The drug-loaded PLA–TPGS NPs were prepared by the dialysis method. Particle size, surface morphology and surface chemistry, *in vitro* drug release and cellular uptake of NPs were characterized. *In vitro* and *in vivo* therapeutic effects of the nanoparticle formulation were evaluated in comparison with Taxol®.
Results. The PLA–TPGS NP formulation exhibited significant advantages in *in vivo* pharmacokinetics and xenograft tumor model *versus* the PLGA NP formulation and the pristine drug. Compared with Taxol®, the PLA–TPGS NP formulation achieved 27.4-fold longer half-life in circulation, 1.6-fold larger area-under-the-curve (AUC) with no portion located above the maximum tolerance concentration level. For the first time in the literature, one shot for 240 h chemotherapy was achieved in comparison with only 22 h chemotherapy for Taxol® at the same 10 mg/kg paclitaxel dose. Xenograft tumor model further confirmed the advantages of the NP formulation *versus* Taxol®.
Conclusions. The PLA–TPGS NP formulation can realize a way of controlled and sustained drug release for more than 10 days, which relieves one of the two major concerns on cancer nanotechnology, *i.e.* feasibility.

KEY WORDS: chemotherapeutic engineering; controlled release; nanomedicine; nanopharmaceutical engineering; paclitaxel.

INTRODUCTION

Paclitaxel is one of the best antineoplastic drugs found from nature in the past decades, which has excellent therapeutic effects against a wide spectrum of cancers including ovarian cancer, breast cancer, colon cancer, small and non-small cell lung cancer, neck cancer and AIDS related Kaposi's sarcoma (1–3). Like many other anticancer agents, paclitaxel has problems in formulation due to its extremely low solubility. Its current clinical dosage form, Taxol®, is formulated in an adjuvant called Cremophor EL, which has been found to be responsible for many serious side effects of Taxol® including hypersensitivity reactions, nephrotoxicity, cardiotoxicity and neurotoxicity (4–6). Research has thus been concentrated on developing alternative dosage forms devoid of Cremophor EL, which include liposomes, micelles, paste and polymeric microspheres and nanoparticles. Among them, nanoparticles of biodegradable polymers may have advantages to solve the formulation problem of paclitaxel as well as to realize a controlled and sustained way for paclitaxel delivery (7,8).

Poly(lactide) (PLA), poly(D,L-lactide-co-glycolide) (PLGA), and poly(caprolactone) (PCL) are FDA-approved biodegradable polymers, which are used most often in the literature for drug delivery and tissue engineering. These polymers are originally synthesized to make medical implants and surgical sutures, and thus may not be as desired for drug formulation due to their high hydrophobicity, slow degradation and ease to be taken by macrophages (9,10).

In the present work, a novel kind of biodegradable copolymers, poly(lactide)-D-α-tocopheryl polyethylene glycol 1,000 succinate (PLA–TPGS) with various PLA/TPGS component ratios was synthesized for nanoparticle formulation of small molecule anticancer drugs with paclitaxel as a model drug. TPGS is a water-soluble derivative of natural vitamin E with amphiphilic structure. It has been used as emulsifier,

[1] Department of Chemical and Biomolecular Engineering, National University of Singapore, Block E5, 02-11, 4 Engineering Drive 4, Kent Ridge, 117576, Singapore.
[2] NUS Nanoscience and Nanotechnology Initiative (NUSNNI), National University of Singapore, Block E3, 05-29, 2 Engineering Drive 3, Singapore 117576.
[3] Division of Bioengineering, National University of Singapore, Block E5, 02-11, 4 Engineering Drive 4, Kent Ridge, 117576, Singapore.
[4] *Present Address*: Harvard University Medical School, Dana-Farber Cancer Institute, 44 Binney Street, Boston, Massachusetts 02115, USA.
[5] *Present Address*: Institute of Chemical and Engineering Sciences, A*STAR, Singapore, Singapore.
[6] To whom correspondence should be addressed. (e-mail: chefss@nus.edu.sg)

solubilizer, bioavailability enhancer of hydrophobic drugs, and colloid drug delivery vehicles. Its wide application is credited to its stability and safety in human bodies. The National Cancer Institute (NCI) conducted a study on the "One-Year Chronic Oral (Incubation) Toxicity Studies in Rats and Dogs" and has concluded that TPGS is safe for oral consumption even at dosages of more than 1 g/kg/day in the animal test (11). Co-administrated TPGS has shown to increase the absorption of vancomycin hydrochloride, cyclosporine, amprenavir, and talinolol by increasing their solubility, permeability and stability (12–15). Moreover, it has been found that co-administration of TPGS with anticancer drugs could enhance their cytotoxicity, inhibit P-glycoprotein mediated multi-drug resistance (MDR), and increase their oral bioavailability (15–17). Our group has creatively used TPGS as a novel kind of emulsifier or additive in preparation of PLGA nanoparticles for drug formulation. TPGS-emulsified PLGA nanoparticles have achieved high emulsification efficiency (67 times higher than PVA), high drug encapsulation efficiency (up to 100% for 10% drug loading) (18,19), high cellular uptake by Caco-2 cells and high cancer cell cytotoxicity for Caco-2 and HT29 cancer cells (20,21). Our preliminary animal test demonstrated that the TPGS-emulsified PLGA nanoparticle formulation could achieve 3.0 times larger of the area-under-the-curve (AUC), and 1.67-fold longer half-life of the drug in the circulation system than Taxol® could do (21). However, there is a disadvantage for the TPGS-emulsified PLGA NPs. The TPGS used as surfactant may be desorbed from the nanoparticle surface in the preparation process due to its weak association with the nanoparticles. This triggered us to synthesize PLA–TPGS copolymers, which have resulted in higher *in vitro* cellular uptake of the nanoparticles and higher *in vitro* cytotoxicity of the formulated drug than the TPGS-emulsified PLGA NPs (22,23).

In our earlier papers, the PLA–TPGS nanoparticles were prepared by the solvent extraction/evaporation single emulsion method (22,23). Alternatively, the nanoparticles can also be prepared by the dialysis method, which needs neither any external energy such as sonication or homogenization for mixing, nor any surfactant to avoid its possible side effects. For example, polyvinyl alcohol (PVA) is a surfactant which is used most often in nanoparticle formulation in the literature, which still needs to be approved by FDA. Our previous *in vitro* investigation demonstrated that except for the advantage in producing nanoparticles of more uniform size, the dialysis method prepares the PLA–TPGS nanoparticles which could increase the Caco-2 cell uptake by 1.4-fold in comparison with the PLGA nanoparticles at 250 mg/ml NP concentration after 2 hour incubation, and the HT-29 cell viability by 1.52 times than Taxol® after 24 h incubation at 25 μg/ml paclitaxel concentration, respectively (24).

In the present work, we continued our research on the PLA–TPGS NP formulation of anticancer drug with paclitaxel as a model drug, which are prepared by the dialysis method, with focus on *in vivo* evaluation in close comparison with the PLGA NP formulation as well as with Taxol®, which include pharmacokinetics, biodistribution and xenograft tumor model. The results obtained will determine if the PLA–TPGS NP formulation could be feasible for cancer treatment as well as for various other biomedical applications, which is one of the main concerns on cancer nanotechnology.

MATERIALS AND METHODS

Materials

Poly(D,L-lactic-co-glycolic acid) (PLGA with L/G molar ratio of 50:50 and Mw of 40,000–75,000) was purchased from Sigma (St. Louis, MO, USA). Paclitaxel was obtained from Dabur India Limited, India. Dialysis membrane (MWCO 3,500) was purchased from Spectrum Laboratories Inc.

Synthesis of PLA–TPGS Copolymers

PLA–TPGS copolymers with various PLA/TPGS component ratios were synthesized by the ring-opening polymerization in the presence of lactide and TPGS. The number molecular weights calculated from NMR were 79,700, 18,900, and 12,700 for PLA–TPGS 98:2, 92:8 and 88:12 copolymers, respectively. PLA-TPGS 98:2, PLA-TPGS 92:8 and PLA-TPGS 88:12 copolymer stands for the copolymer of the 98:2, 92:8, 88:12 weight ratio between the PLA and TPGS components, respectively. The readers are referred to our earlier paper for details of the PLA–TPGS copolymer synthesis and characterization (22).

Preparation of Paclitaxel-loaded PLA–TPGS Nanoparticles

The drug loaded PLA–TPGS NPs used in this work were prepared by the dialysis method (24). In brief, the weighed paclitaxel and PLA–TPGS copolymer were dissolved in a suitable solvent, which is also a parameter under investigation, at a specified concentration. For instance, an amount of 50 mg of PLA–TPGS copolymer with 10 wt% of paclitaxel were dissolved in 20 ml of *N*,*N*-dimethylformamide (DMF) to have a concentration of 2.5 mg/ml solvent and the solution then was dialyzed against Millipore water for 30 h with changing water once every 3 h. The nanoparticles were collected after filtration, centrifugation for 20 min at 14,000×*g* and freeze-drying for 2 days.

Characterization of Nanoparticles

Particles Size, Surface Morphology and Surface Chemistry

Particle sizer system from Brookhaven Instruments Corporation, 90 Plus was used to analyze the size of the nanoparticles fabricated. The surface morphology was investigated by the field emission scanning electron microscopy (FESEM). The XPS (X-ray photoelectron spectroscopy) was used to analyze the surface chemistry of the drug-loaded nanoparticles.

Drug Encapsulation Efficiency

Paclitaxel-loaded nanoparticles dissolved in DCM was evaporated at nitrogen atmosphere and then reconstituted at mobile phase of 50/50 *v*/*v* acetonitrile/water solution. Paclitaxel entrapped in the nanoparticles was measured by HPLC (Agilent LC 1100) (22). Agilent® eclipse XDB-C18 column (4.6×250 mm i.d., pore size 5 μm) was used for chromatographic separation and UV detection was performed at 227 nm in HPLC system.

In Vitro Drug Release

Four milligrams of the paclitaxel-loaded nanoparticles were weighed and dispersed into 10 ml of PBS with 0.1% Tween 80 in a centrifuge tube. The tubes were placed in an orbital shaker water bath (GFL-1086, Lee Hung Technical Company) at a temperature of 37°C and orbiting speed of 120 rpm. At allocated time intervals, the tubes were centrifuged at a speed of 14,000×*g* for 20 min. After centrifuging, the PBS supernatant was pipetted out into screw capped tube while a fresh 10 ml of PBS was added to the nanoparticles and redispersed before replacing them in the orbital shaker water bath. The supernatant was extracted with 2 ml DCM and reconstituted in 3 ml mobile phase for HPLC analysis.

Cellular Uptake

HT-29 cells (a human colon adenocarcinoma cell line) were cultured in DMEM (prescribed in 10% FBS and 1% antibiotic–antimycotic) and incubated in SANYO CO_2 incubator at 37°C in a humidified environment of 5.0% CO_2. The cells were harvested with 0.125% of Trypsin–EDTA solution and then seeded at a density of 6.5×10^4 cells/well in 96-well black plates (Costar, Corning, NY) for quantitative cellular uptake analysis. After the cells reached confluence, they were equilibrated with HBSS at 37°C for 1 h and then the cells were incubated with coumarin-6 loaded nanoparticles suspension at 37°C for 2 h. The experiment was terminated by washing the cell monolayer three times with cold PBS to remove any nanoparticles not taken up by the cells. Fifty microliters of triton was then introduced into each well to lyse the cells. The fluorescence intensity of each sample well was measured using a microplate reader (GENios, Tecan, Switzerland, λ_{ex}=430 nm and λ_{em}=485 nm). Cell uptake efficiency was expressed as the percentage of cells associated fluorescence *versus* the fluorescence present in the feed solution. For qualitative study, cells were reseeded in the LAB-TEK chamber and washed for four times after incubated with coumarin 6-loaded nanoparticles for 2 h. The cells were washed twice with cold PBS after fixed by ethanol and then the nuclei were counterstained with propidium iodide (PI). The cell monolayer was observed by confocal laser scanning microscope (CLSM, Zeiss LSM 410) with an imaging software (Fluoview FV500).

Animal Test

The animal experiment protocols of this research were approved by the Institutional Animal Care and Use Committees (IACUC, Protocol #: 802/05), Office of Life Science, National University of Singapore. Male Sprague–Dawley (SD) rats of 150–200 g and 4–5 week old were supplied by the Laboratory Animals Centre of Singapore and were maintained at the Animal Holding Unit of National University of Singapore. Severe combined immunodeficient (SCID) mice of 15–20 g were supplied by the Jackson Laboratory, Maine, USA and were maintained under specific pathogen-free status (22±2°C, R.H.=60–70%).

Pharmacokinetics and Biodistribution

The SD rats were randomly assigned to two groups of 13 rats for pharmacokinetics and biodistribution investigation. Group 1 and 2 received an i.v. injection of Taxol® or the paclitaxel-loaded PLA–TPGS 88:12 nanoparticles, respectively at an equivalent dose of 10 mg/kg paclitaxel *versus* the body weight, respectively. The drug-loaded nanoparticle suspension or Taxol® were diluted with saline to have around 1 ml injection volume and administrated through tail vein. All animals were observed for mortality, general condition, body weight and potential clinical signs. Blood samples were collected at 0 (pre-dose), 0.25, 0.5, 1, 2, 4, 8, 12 and 24 h after administration of Taxol® from four rats. After administration of nanoparticles, blood samples were collected at 0 (pre-dose), 1, 2, 4, 8, 12, 24, 48, 72, 108, 168, 240 h. Plasma samples were harvested by centrifugation at 14,000×*g* for 10 min and then stored at −20°C for HPLC analysis. To examine the biodistribution of paclitaxel, three rats were anesthetized at the assigned time intervals (1, 4 and 24 h) post-injection and organs (liver, spleen, brain, kidney, lung, small intestine and stomach) were harvested and cleared of blood. The tissues were freeze-dried and then ground manually into powder for easy extraction before they were transferred into Eppendorf tubes.

Liquid–liquid extraction was performed prior to analysis. The samples were extracted with 1 ml of ethyl acetate on a vortex-mixer for 90 s. Upon centrifugation at 14,000×*g* for 15 min, 0.9 ml of the organic layer was transferred to another batch of 1.5 ml clean Eppendorf tubes and evaporated under nitrogen atmosphere at room temperature. The residue was reconstituted with 100 μl of mobile phase b (acetonitrile/methanol/water=40/5/55 *v*/*v*/*v*) and then centrifuged at 14,000×*g* for 15 min. Eighty microliter of the clear upper layer was transferred to autosampler vials containing limited-volume inserts (100 μl) before analyzed by HPLC. The mobile phase consisted of mobile phase a (acetonitrile/methanol/water=45/5/50 *v*/*v*/*v*) and b with linear gradients of 100% mobile phase b to 0% in 50 min, then linear gradients to 100% mobile phase b in 1 min, then 100% mobile phase b held for 4 min and was delivered at a flow rate of 1.0 ml/min.

Non-compartmental analysis was done using *Kinetica* Software (Thermo Electron Corporation, USA). The maximum paclitaxel concentration (C_{max}) and the corresponding time (t_{max}) were observed values. The elimination constant (λ_n) was obtained by log-linear regression analysis of the terminal phase of the whole blood concentration *versus* time profile. The elimination half-life ($t_{1/2}$) was calculated as ln (2/λ_n). The area under the concentrations *versus* time curve (AUC_{last}) and area under the first moment curve from time 0 to the last measured concentration ($AUMC_{last}$) were calculated by log-linear trapezoid rule. The AUC of toxic level (AUC_{toxic}) was calculated as that at the drug concentration higher than 8,540 ng/ml. The AUC of extrapolated area (AUC_{extra}) was estimated by dividing the last measured concentration by λ_n. AUC_{extra} was added to AUC_{last} to estimate AUC from time 0 to infinity (AUC_{inf}). AUMC from 0 to infinity ($AUMC_{inf}$) was estimated as $AUMC_{last}+C_{last}/(\lambda_n)^2+C_{last}t_{last}/\lambda_n$. Mean residence time was calculated as $AUMC_{inf}/AUC_{inf}$.

Xenograft Tumor Model

About 0.1 ml of HT-29 cells in the culture medium was injected via 27-gauge needle into the subcutaneous (s.c.) space of right flank region of the mouse at a dosage of 2×10^6 cells/mouse. After inoculation of HT-29 cells, the s.c. tumor growth in each mouse was closely observed. The tumor volume can be calculated from the formula: $0.524\times(\text{length})\times(\text{width})^2$. When the tumor volume reaches about 100–200 mm^3, the mice were randomly divided into three groups, which were subject to intra-tumoral injection of the saline as a control and the PLA–TPGS 88:12 nanoparticle formulation or Taxol®, respectively at 10 mg/kg paclitaxel dose. All mouse behaviors and clinical signs were closely observed. Tumors were measured from time to time. Anti-tumoral injection was given at day 0, 4, 8 and 24.

RESULTS AND DISCUSSION

Formulation Optimization

The paclitaxel-loaded PLA–TPGS nanoparticles were prepared by the dialysis method without using any surfactant. The formulation optimization was pursued and the results were shown in Table I, II, III, IV, which show the effects of the organic solvent type, the copolymer concentration in the organic solvent, the drug loading in the nanoparticles, and the PLA/TPGS component ratio of the copolymer on the characteristics of the nanoparticle formulation.

The organic solvent used to dissolve the PLA–TPGS copolymers can affect the particle properties through the copolymer solubility in the solvent, the diffusion rate of the solvent into the aqueous phase, the solvent–water miscibility, and the solubility of the drug in the solvent (25). To investigate such effects, various water miscible solvents such as DMF, acetone, 1,4-dioxane, acetonitrile, DMSO and THF were used in the present work. As seen in Table I, the DMF showed an acceptable drug encapsulation efficiency (EE) of the nanoparticles, that is 54.0% for 10% drug loading, for which the drug loading efficiency (DLE 32.3%) is higher than the acetone (23.7%), DMSO (27.5%) and 1,4-dioxane (24.3%) and not much lower than THF (39.4%) and acetonitrile (41.7%). However, DMF seems to have resulted in the smallest particles size, 455 nm, which is much smaller than that shown in the acetone, DMSO, 1,4-dioxane, THF and acetonitrile rows. This can be attributed to the differences in the solubility and the miscibility between the copolymer and the solvent, the solvent miscibility with water, the solvent viscosity, and other properties of the solvent. The particles size and size distribution play an important role in determining the *in vitro* drug release kinetics and cellular uptake as well as the *in vivo* biodistribution of the nanoparticles, and thus the therapeutic effects of the drug-loaded nanoparticles. Due to the porosity of the tumor vasculature and the lack of lymphatic drainage, colloidal nanoparticles are preferentially distributed in the tumors due to the enhanced permeability and retention effect (EPR) (26,27). Therefore, to achieve as small as possible particles size with acceptable drug encapsulation efficiency, we chose DMF as the organic solvent in the following experiments.

The possible effects of the copolymer concentration in the organic solvent on the particles size and drug encapsulation efficiency (EE) were also investigated. As shown in Table II, it appeared that the lower the copolymer concentration, the smaller the particles size would be achieved. The particle size was increased from 367 to 475 nm as the polymer concentration in DMF was increased from 2.5 to 15 mg/ml. This could be understood since the copolymer and the drug can be better dispersed in a more dilute environment and thus unlikely to aggregate to form larger particles. Also, higher polymer concentration results in higher viscosity, which leads to lower diffusion rate of the solvent and thus results in larger particle size (28). There was no significant difference in the drug EE. The PLA–TPGS nanoparticles

Table I. Effects of Different Organic Solvents on Nanoparticle Formulation

Solvent	Particle size (nm)	EE[a] (%)	DLE[b] (%)
DMF	455±5	54.0±4.7	32.3±4.5
Acetone	763±37	86.0±6.8	23.7±4.0
DMSO	608±20	67.4±2.3	27.5±2.0
Dioxane	794±67	88.0±8.6	24.3±3.2
THF	1,102±90	89.1±5.6	39.4±4.0
Acetonitrile	818±55	73.2±6.3	41.7±3.7

Polymer is PLA–TPGS 92:8; polymer concentration=12.5 mg/ml; drug loading=10%.

[a] $EE=\frac{\text{actual drug loading \% in nanoparticles}}{\text{theory drug loading \% in nanopaarticles}}\times100\%$

[b] $DLE=\frac{\text{actual drug amount loaded in nanoparticles}}{\text{theory drug amount added in fabrication}}\times100\%=EE\times\text{recovery of nanoparticles}$

Table II. Effects of Copolymer Concentration in DMF on Nanoparticle Formulation

Copolymer concentration (mg/ml)	Particle size (nm)	EE (%)	DLE (%)
2.5	367±12	60.2±3.2	48.8±3.2
5.0	437±21	60.5±2.2	45.9±2.7
10.0	452±18	53.2±3.7	33.9±5.0
12.5	455±5	54.0±4.7	32.3±4.5
15.0	475±28	56.5±3.5	35.0±2.7

Polymer is PLA–TPGS 92:8; drug loading=10%.

Table III. Effects of Different Drug Loading on Nanoparticle Formulation

Theory drug loading (%)	Particle size (nm)	EE (%)	DLE (%)
0	327±13	N.A.	N.A.
1.0	327±21	88.6±5.2	53.1±3.5
2.5	324±10	79.5±3.1	49.4±3.2
5.0	356±15	68.3±2.7	44.6±3.1
10.0	367±12	60.2±3.2	48.8±3.2
20.0	452±20	24.6±4.1	11.5±5.0

Polymer is PLA–TPGS 92:8; polymer concentration in DMF=2.5 mg/ml.
N.A.: not applicable

Table IV. Effects of Different PLA/TPGS Component Ratio on Nanoparticle Formulation

Polymer	Particle size (nm)	EE (%)	DLE (%)
PLGA	437±25	54.7±6.8	31.7±1.8
PLA–TPGS 98:2	423±27	53.1±5.7	27.1±2.1
PLA–TPGS 92:8	367±12	60.2±3.2	48.8±3.2
PLA–TPGS 88:12	343±19	51.8±4.9	45.9±3.2

Polymer concentration in DMF=2.5 mg/ml; drug loading in nanoparticles=10%.

prepared with 2.5 mg/ml copolymer concentration in DMF achieved the highest drug loading efficiency (DLE) up to 49%. DLE is another important factor since anticancer drugs such as paclitaxel are usually expensive, which can also directly affect the amount of the drug-loaded nanoparticles at a given dose. When we disperse the nanoparticle formulation in a given volume of saline for i.v. administration, the required amount for the 1% drug-loaded nanoparticles would be six times of that for the 6% drug-loaded nanoparticles. In our experience, however, the nanoparticle concentration in saline can not be higher than 30 mg/ml for the safety reason. Therefore, we have to get higher EE and DLE in the nanoparticle formulation and the optimized copolymer concentration was thus selected to be 2.5 mg/ml.

The EE and particles size were also affected by the theoretical drug loading. As seen from the Table III, the EE was decreased as increasing the drug loading (drug feed). Especially, the EE was decreased greatly from 60.2% for 10% drug loading to 24.6% for 20% drug loading. This is natural since the higher drug loading, the lower the EE could be resulted as found by other researchers (25,29). For a given polymer/copolymer, there may be a limitation for the EE. The particles size was increased significantly from 367 nm for 10% drug feed to 452 nm for 20% drug feed. It seems that an appropriate drug feed in preparation of the PLA–TPGS nanoparticles should be 10% and the actual loading is around 6%.

A comparison was between the PLA–TPGS nanoparticles and the PLGA nanoparticles, which are used most often in the literature. As seen from Table IV, the particles size was decreased from 437 nm for the PLGA nanoparticles to 343 nm for the PLA–TPGS 88:12 nanoparticles under the same preparation conditions. It seems that the lower the PLA/TPGS ratio is (*i.e.* the more TPGS contained in the copolymer), the lower molecular weight or the viscosity of the organic phase would be obtained, which may thus result in smaller particles size.

Surface Morphology, Surface Chemistry and *In Vitro* Drug Release

As seen from Fig. 1a, the PLA–TPGS nanoparticles exhibited spherical shape of moderate uniform particles size. The particles size measured from the FESEM images were found in good agreement with that measured by the laser light scattering technique.

Surface chemistry of the drug-loaded PLA–TPGS nanoparticles was investigated by XPS, which was carried out to find what component is dominated on the nanoparticle surface by making use of the corresponding characteristic bonds. We found from XPS N1s (atomic orbital 1 s of nitrogen) region that no nitrogen element signal could be detected on the surface of the paclitaxel-loaded PLA–TPGS nanoparticles, which means that paclitaxel was successfully encapsulated inside the nanoparticles (data not shown). The XPS C1s region of the pure copolymer and the drug-loaded PLA–TPGS 92:8 copolymer nanoparticles was shown in Fig. 1b. The peak at the 286.1 eV (C–O–C bonds) can be regarded as the indicator of the TPGS component of the copolymer. It can be seen from Fig. 1b that the peak ratio of the C–O–C bonds is increased from 14% for the pure PLA–TPGS copolymer to 22% for the drug-loaded PLA–TPGS nanoparticles. This demonstrated the presence of TPGS on the particles surface.

Fig. 1c shows the *in vitro* drug release profile of the paclitaxel-loaded PLA–TPGS nanoparticles in comparison with that of the paclitaxel-loaded PLGA nanoparticles. It can be seen that the paclitaxel-loaded PLGA nanoparticles and the PLA–TPGS 98:2, 92:8 and 88:12 nanoparticles displayed an initial burst up to 24.0%, 23.0%, 29.7% and 31.1% drug release in the first day, and 63.6%, 60.0%, 77.7% and 80.3% accumulated drug release after 30 days, respectively. The PLA–TPGS nanoparticles have faster drug release than the PLGA nanoparticles, and the lower the PLA/TPGS ratio (the more TPGS component) showed the faster drug release. This may be caused by the greater hydrophilic characteristic and thus the faster degradation rate of the PLA–TPGS copolymers of lower PLA/TPGS ratio. Similar results of a more hydrophilic composition effect on *in vitro* drug release were also reported by other researchers (25,30).

It is important to reserve a sink condition for the *in vitro* drug release experiment. As mentioned in the "Materials and Methods" section, we added 4 mg nanoparticles of 10% drug loading with 60% drug encapsulation efficiency into 10 ml PBS. The maximum drug concentration in the release medium could have been 24 μg/ml if all drug molecules in the nanoparticles were released in the same 10 ml PBS medium. Nevertheless, we took the release medium out of the sample tube frequently at 3, 6, 12 and 24 h on the first day and everyday afterwards, and each time we did so, another 10 ml fresh medium was added into the tube for continuous measurement of the accumulative drug release. The sink condition was thus well maintained.

Cellular Uptake of Nanoparticles

Fig. 2a shows the HT-29 cell uptake efficiency of the coumarin-6-loaded PLGA and PLA–TPGS nanoparticles after 2 h incubation at 250 μg/ml nanoparticle concentration. We can see from this figure that the cellular uptake efficiency was enhanced 1.6 times for PLA–TPGS 92:8 nanoparticles and 1.8 times for the PLA–TPGS 88:12 nanoparticles in comparison with the fluorescent PLGA nanoparticles, respectively. Nevertheless, the PLA–TPGS 98:2 nanoparticles did not show any significant enhancement in the cellular uptake, which may be due to too little TPGS in the copolymer. This result is consistent with that found from the TPGS-coated PLGA nanoparticles in earlier work of our group, where the TPGS-coated PLGA nanoparticles were found to enhance the Caco-2 cell uptake efficiency by 1.3 times in comparison with the PVA-coated PLGA nano-

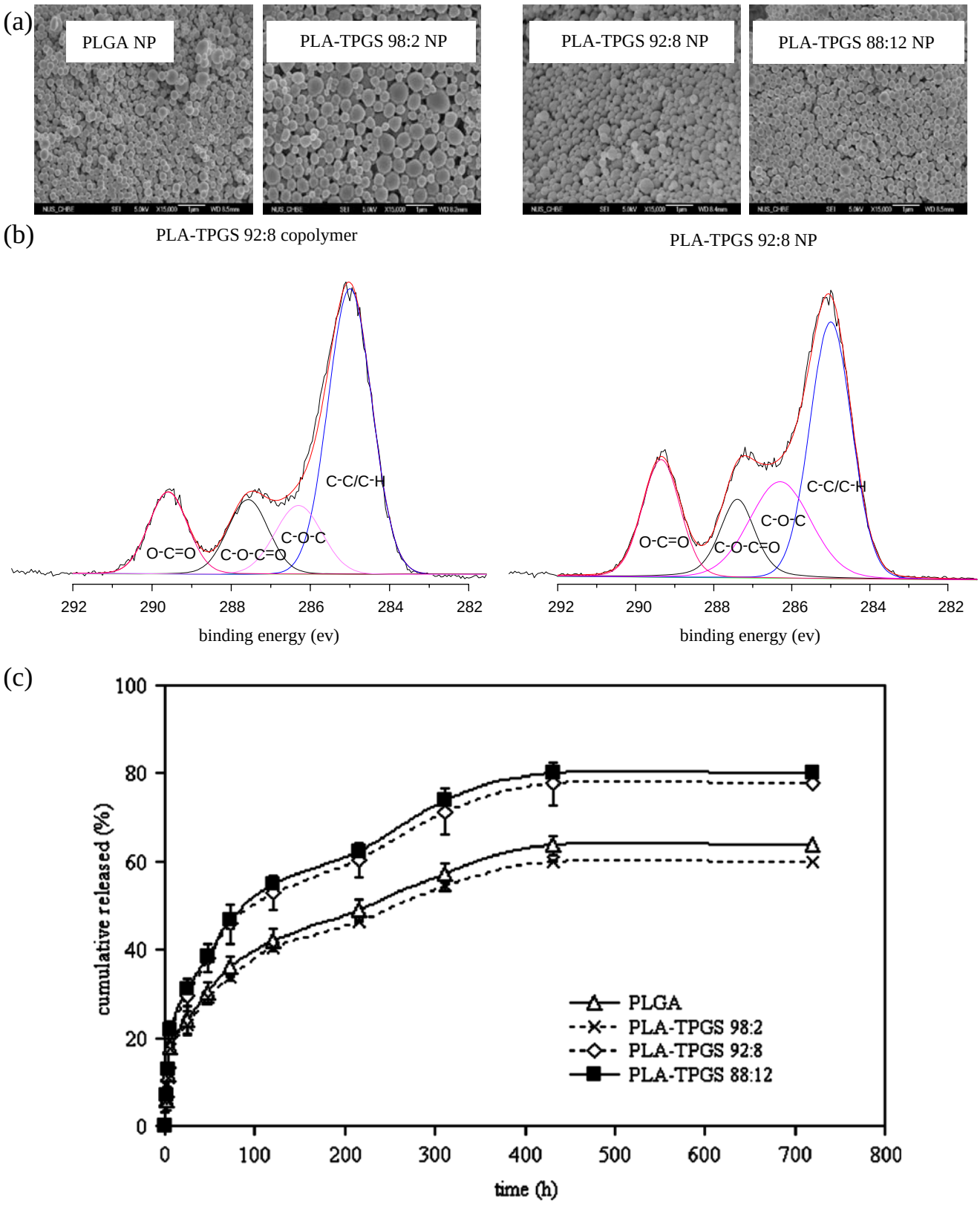

Fig. 1. **a** FESEM images, **b** XPS spectra and **c** *in vitro* drug release in PBS at 37°C of the paclitaxel-loaded PLA–TPGS nanoparticles. Data represents mean±SD, $n=3$.

particles (20). In comparison with our earlier work on the TPGS-emulsified PLGA nanoparticles, the PLA–TPGS nanoparticles can take more advantage of the TPGS absorption stability on the surface of nanoparticles, which can be controlled by adjusting the PLA/TPGS ratio of the PLA–TPGS copolymers. At the mean time, we can see from the confocal microscopic images of Fig. 2b that the coumarin 6-loaded nanoparticles (green) are closely around the nuclei

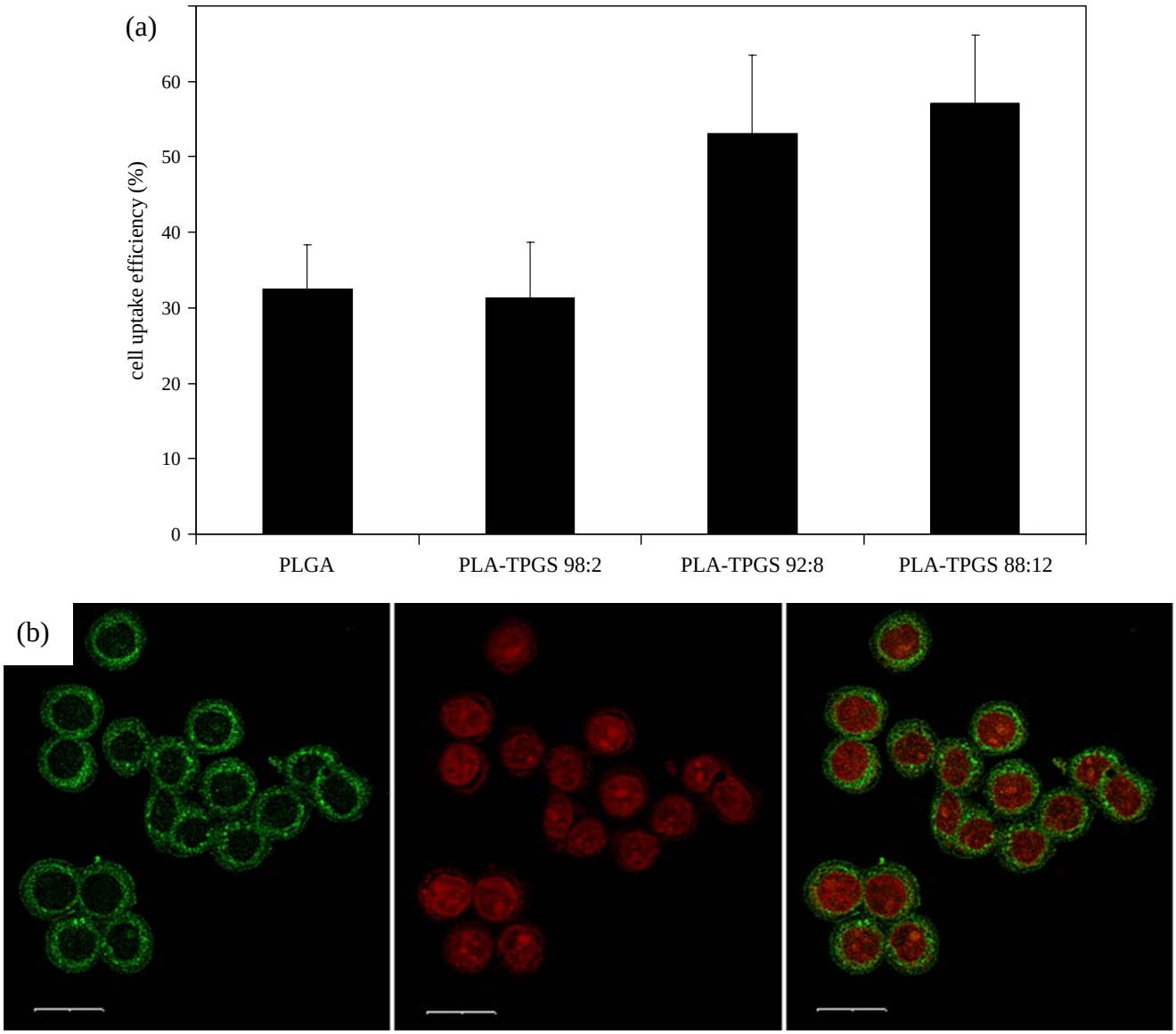

Fig. 2. Cellular uptake of coumarin 6-loaded PLA–TPGS nanoparticles prepared by the dialysis method after incubated with HT-29 cells for 2 h at 250 μg/ml nanoparticle concentration. **a** Cell uptake efficiency of the coumarin-loaded PLGA nanoparticles and PLA–TPGS nanoparticles (n=6). **b** Confocal microscopic images of HT-29 cells after incubated with PLA–TPGS nanoparticles (*green*). The nuclei were stained by propidium iodide (*red*) and the images were obtained by FITC (*left*) and RITC (*middle*) filter and overlapped FITC and PI channel (*right*). Bar presents 20 μm.

(red), which confirms the uptake of nanoparticles by the cells, some can even penetrate into the nuclei.

There may be a few important questions to doubt the above experiment. (1) Are the fluorescent nanoparticles located inside the cells or just adhered on the cell surface? (2) Where does the signal actually come from, the nanoparticles inside the cells or the free coumarin released from the nanoparticles adhered on the cell surface? (3) Is the fluorescence located in the cytoplasm or outside the cells since cancer cells may be full by their nucleus? We conducted two extra experiments in our earlier publications to image the cells cultured with the released medium used for the *in vitro* drug release experiment and to measure the fluorescence release kinetics from the nanoparticles in the cell culture medium. We found that the control experiments performed by incubating the cells with medium of the coumarin-6 released from the nanoparticles did not show any significant uptake, which demonstrated that the raw coumarin-6 markers cannot be directly internalized by the cells (20). We also found that the coumarin-6 was released only less than 3.75% over 24 h incubation time, which was considered negligible in comparison with the nanoparticle uptake outcome of the cells (20). It is thus reasonable to assume that most of the coumarin-6 was associated inside the nanoparticles and the fluorescence measured from the uptake samples mainly reflects the fluorescent nanoparticles inside the cells but not the released fluorescence in the medium.

By the way, it should be pointed out that the CLSM has sectioning function. The images show the fluorescence distribution across the cross section but not the cell surface.

Furthermore the cellular uptake of the nanoparticles have been confirmed by the cryo-SEM and TEM images of the cells cultured for 1 h with the medium (20).

Pharmacokinetics

Fig. 3a shows the pharmacokinetics (PK) of paclitaxel formulated in the PLA–TPGS nanoparticles in comparison with that of Taxol® after i.v. administration to SD rats at the same 10 mg/kg paclitaxel dose (n=4). The maximum tolerable level and minimum-effective level are 8,540 and 43 ng/ml, respectively (31). We can see from this figure that the PLA–TPGS NP formulation achieved much better therapeutic effects indicated by the much larger AUC and much longer half-life in comparison with Taxol®.

The major pharmacokinetic parameters of the PLA–TPGS NP formulation were obtained by the non-compartmental analysis, which was made in close comparison with those of the Taxol® administration at the same 10 mg/kg paclitaxel dose. The results are listed in Table V. It can be seen from this table that the PLA–TPGS 88:12 nanoparticle formulation would have much less side effects than Taxol® since it has no AUC located above the maximum tolerable level. On the contrast, 39.9% of the total AUC for the Taxol® administration was located above the 8,540 ng/ml line, which should be responsible for the serious side effects of Taxol®. Moreover, the total AUC for the PLA–TPGS 88:12 nanoparticles formulation was 79,100 ng h/ml, which is 1.6-fold of 50,900 ng h/ml for Taxol® at the same 10 mg/kg paclitaxel dose. This means the PLA–TPGS 88:12 nanoparticle formulation could achieve 1.6 times of the therapeutic effects compared with Taxol®. As the half-life of the drug in the plasma regards, the value for the PLA–TPGS 88:12 NP formulation was found to be 76.8 h, which is 27.4 times of 2.8 h for Taxol® at the same 10 mg/kg paclitaxel dose. Equivalently, we can find from Table V or Fig. 3a that the PLA–TPGS 88:12 nanoparticle formulation achieved much longer effective treatment period and one shot for 224.5 h sustainable chemotherapy was achieved. In comparison, only 22.9 h chemotherapy can be realized for Taxol® at the same 10 mg/kg paclitaxel dose. This indicates that the PLA–TPGS nanoparticle formulation is promising for sustainable chemotherapy up to 224.5 h (around 10 days).

There have been two main concerns on the emerging cancer nanotechnology: feasibility and safety. Our results have proved the feasibility and the biodegradable nature of our PLA–TPGS nanoparticles should cause much less problems in safety in comparison with non-degradable nanoparticles such as metal and inorganic nanoparticles.

Biodistribution

Fig. 3c shows the biodistribution of paclitaxel in the blood and various tissues such as spleen, liver, stomach, intestine, kidney, lung and brain 1, 4, 24 h after i.v. injection of the PLA–TPGS NP formulation in close comparison with that of Taxol® at the same 10 mg/kg paclitaxel dose as shown in Fig. 3b. The Taxol® administration showed a high drug concentration in the various organs at 1 h, *i.e.* 19.711 μg/ml in the blood, 13.224 μg/g in the liver, 5.549 μg/g in the spleen, 7.345 μg/g in the kidney, and 5.555 μg/g in the lung. The rank

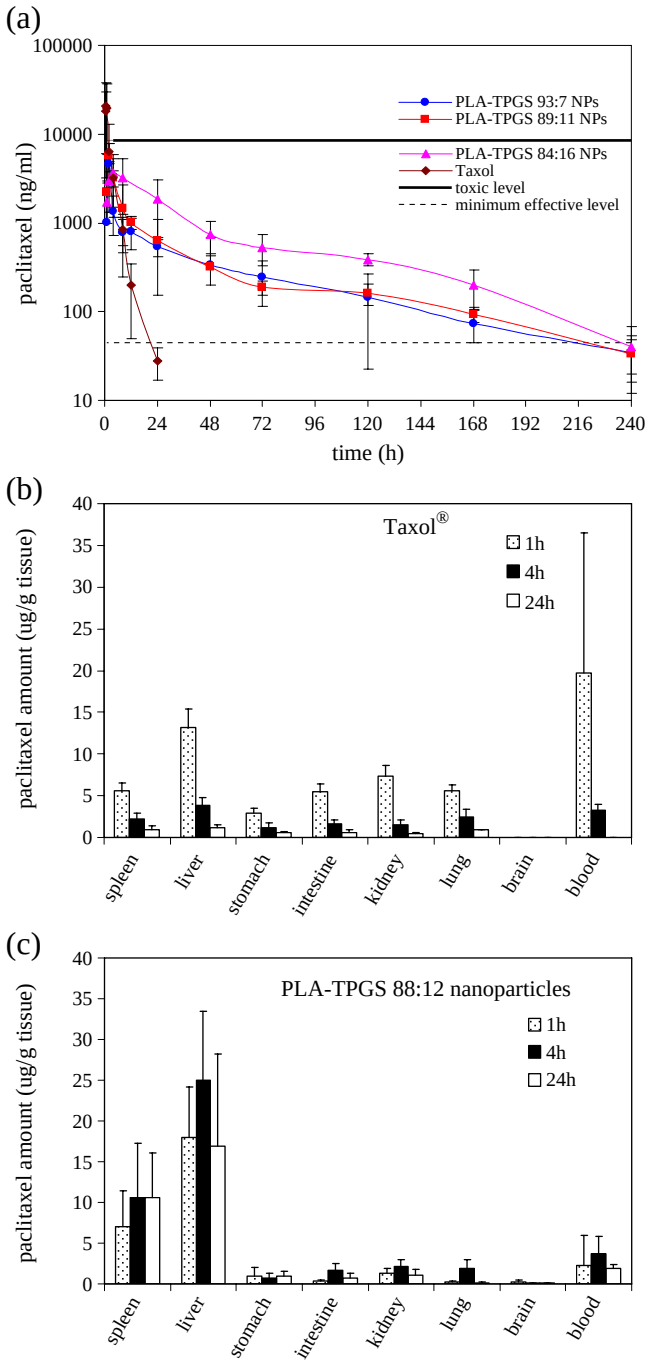

Fig. 3. Pharmacokinetics and biodistribution of paclitaxel formulated in the PLA–TPGS nanoparticles in comparison with those of Taxol® after i.v. administration to SD rats at the same 10 mg/kg paclitaxel dose. **a** Pharmacokinetics. The maximum tolerable level and minimum-effective level are 8,540 and 43 ng/ml, respectively (31) (n=4). **b** and **c** Biodistribution profiles of the drug formulated in Taxol® (**b**) and PLA-TPGS 88:12 nanoparticles (**c**) in SD rats 1, 4, 24 h after i.v. injection (n=3).

order of the drug levels for the Taxol® formulation was blood>liver>kidney>lung>spleen>intestine>stomach> spleen>blood>kidney>lung>intestine>stomach>brain. The drug level in the organs and the blood was decreased as the time went on. These results are similar to those obtained for other nanoparticle formulations in the literature (32,33).

Table V. Pharmacokinetic Parameters after i.v. Injection of the PLA–TPGS 88:12 Nanoparticles or the Taxol® Formulation at a Dose of 10 mg/kg Paclitaxel

Variable	C_{max} (ng/ml)	t_{max} (h)	$t_{1/2}$ (h)	t_{st} (h)	AUC_{inf} (ng·h/ml)	MRT (h)	$\%AUC_{toxic}$
PLA–TPGS NPs	5,770±2,740[a]	2.0	76.8±15.3[a]	224.5±20.7[a]	79,100±13,800	69.0±11.2[a]	0
Taxol®	20,700±12,100	0.5	2.8±0.7	22.9±1.2	50,900±20,900	2.6±0.5	39.9±7.2
NPs/Taxol®	–	–	27.4	9.8	1.6	26.5	–

t_{st}: sustainable therapeutic time at which the drug concentration in the plasma dropped below the minimum effective level (43 ng/ml for paclitaxel)
[a] Points which the values for NPs were statistically different from Taxol® using ANOVA at a confidence interval of 95%.

It should be noticed that a significant portion of drug was found accumulated in the liver and spleen, which may be due to the mononuclear phagocytosis system (MPS) existing especially in the liver and spleen (32). Moreover, the nanoparticle formulation demonstrated relatively high drug level in the brain compared with Taxol®. It is well known that paclitaxel can not reach the brain after i.v. administration because of the blood brain barrier (BBB) and thus the drug level in brain was not detectable by HPLC for Taxol®. Nevertheless, the drug formulated in the PLA–TPGS NPs reached 0.237 μg/g concentration in the brain 1 h after i.v. administration and still detectable 24 h after the i.v. administration, which was 0.106 μg/g. This may occur since the PLA–TPGS nanoparticles can realize a firm TPGS coating on the nanoparticle surface as shown in Fig. 1b for the surface chemistry analysis of the PLA–TPGS NPs and TPGS has been found to inhibit the P-gp activity which also contributes to the blood brain barrier (34).

Many publications have shown that the circulation half-life of the drug formulated in the PLA-PEG nanoparticles of 100–150 nm diameter was about 2–4 h. In comparison, paclitaxel formulated in our PLA–TPGS nanoparticles of 350–450 nm diameter was 76.8 h. What are the possible reasons that make the PLA–TPGS so much better than PLA-PEG nanoparticle? As we can understand, particle size and surface coating are the two most important factors, which affect the recognition and elimination of nanoparticles by microphages. TPGS is a PEGylated vitamin E, which can greatly reduce the RES effect and thus protect the existent of the nanoparticles in the blood system. This is not a surprise since it has been reported that TPGS can be used to improve oral bioavailability of anticancer drugs such as paclitaxel.

Xenograft Tumor Model

The anti-tumor efficacy of paclitaxel formulated in the PLA–TPGS nanoparticles was investigated on severely combined immunodeficient (SCID) mice of an average body weight of ~16.4 g and an average initial tumor volume of ~108 mm^3. The average tumor growth rate and the animal survival rate were shown in Fig. 4a and b, respectively in close comparison with those of the control (saline only) and the Taxol® formulation.

We can see from Fig. 4a that the PLA–TPGS NP formulation and Taxol® significantly slowed down the tumor growth rate compared with the control. The treatment of the PLA–TPGS NP formulation, Taxol®, and the saline was conducted on day 0, 4, 8 and 24. It seems that time is needed for the drug to be effective in suppressing the tumor growth. It can bee seen that the PLA–TPGS NP formulation group showed the slowest tumor growth rate among the three groups. From day 13 onwards, the advantage of the PLA–TPGS NP formulation *versus* Taxol® became significant. Despite intra-tumoral injection on day 24, no sign of tumor suppression was observed for the Taxol® group. On the contrary, the tumors treated with the PLA–TPGS NP formulation still showed regression on day 24 to day 28 even though the tumor size was increasing after day 28. From the final injection, the drug resistance of the tumor for the Taxol® group was becoming even more obvious compared with the PLA–TPGS NP formulation group. By considering the overall slope of all the curves in Fig. 4a, it can be concluded that the paclitaxel-loaded PLA–TPGS nanoparticles have significant advantages than Taxol® in suppressing tumors. Furthermore, from the analysis of variance (ANOVA) with a confidence interval of 95%, most experimental data points obtained for the PLA–TPGS NP

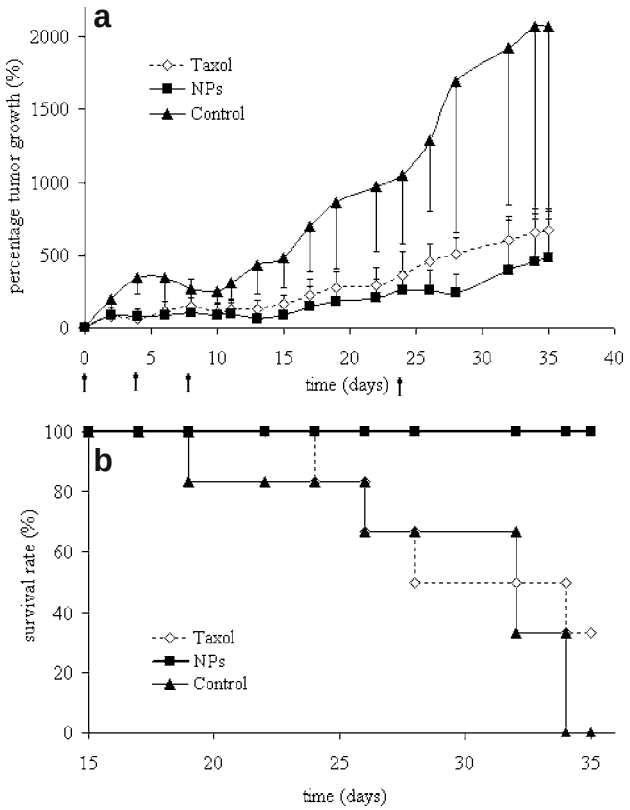

Fig. 4. Antitumor effect of paclitaxel formulated in the PLA–TPGS nanoparticles in comparison with Taxol®. **a** Percentage tumor growth and **b** survival rate of the SCID mice with HT-29 xenograft tumor model after multiple treatment of the same dose. The arrow showed the days when i.v. injections were conducted (n=7).

formulation group after day 13 were found to be statistically significantly different from those for the Taxol® group. In 35 days, Taxol® showed about 503% growth in tumor volume while tumors treated with the PLA–TPGS nanoparticle formulation experienced only 244% tumor growth. In other words, the PLA–TPGS nanoparticle formulation showed about two times more effective than Taxol® in controlling tumor growth. Although no formulation showed successful treatment of HT-29 tumors *in vivo* in the literature, the PLA–TPGS nanoparticle formulation did demonstrate its potential efficacy in controlling the tumor growth.

Survival rate of the tumor-bearing mice represents another important consideration in the *in vivo* evaluation of the various drug formulations. The survival rate was presented in the form of the Kaplan–Meier curve as shown in Fig. 4b. It can be seen from this figure that the group treated with Taxol® has a lower survival rate, *i.e.* ~33.3% on day 35, which may be due to the severe adverse effects of the Taxol® formulation. In contrast, all animals of the group treated with the PLA–TPGS nanoparticle formulation were still alive, *i.e.* 100% survival rate on day 35. Moreover, it is worthy to observe the daily activities, movements, behaviors, which are also important gestures or signals of distress and discomfort caused by the treatment. In fact, some mice in the PLA–TPGS nanoparticle formulation group started showing hemorrhage on their skin surface on day 13 with obvious decrease in tumor size. The mice were still active in their behaviors compared with those in the other two groups, *i.e.* the control group and the Taxol® group. The wound showed signs of improvement, which may due to the immune deficiency of the SCID mice, resulting in slow wound healing. As we can guess, the hemorrhage might be resulted by a combinatory effect of tumor necrosis and the higher cytotoxicity of the PLA–TPGS nanoparticle formulation that led to rapid cell death. Meanwhile, on day 24, another tumor about the same size with the original tumor appeared on opposite side of the dorsal flank of one animal of the Taxol® group, which was related to metastasis of the HT-29 cancer cells. Moreno *et al*. demonstrated that nude mice injected with well-established HT-29 cells or more metastatic variant HT-29 MMM cells showed metastasis from spleen to liver (35). Taxol® was believed to induce an inflammatory response, which was responsible for metastasis of breast cancer cells in the mice (36). The activation of nuclear factor-kappa B (NF-κB) by the inflammation, a transcription factor usually expressed in human cancer cells, which in turn altered the gene expression of the cancer cells, resulted in increasing risk of cancer metastasis. Although the probability of Taxol® to induce inflammation and thus metastasis remain a challenging hypothesis to be proven, it can be deduced, at least from our *in vivo* study, that the PLA–TPGS formulation of paclitaxel does have advantages *versus* the Taxol® formulation with much higher efficacy and much lower side effects including causing metastasis.

CONCLUSIONS

This work is focused on *in vivo* evaluation of the PLA–TPGS nanoparticle formulation of paclitaxel as a model anticancer drug, which includes pharmacokinetics, biodistribution and xenograft tumor model and was conducted in close comparison with Taxol®. The PLA–TPGS nanoparticles were prepared by the dialysis method with formulation optimization of the organic solvent type, the polymer concentration in the organic solvent, the drug loading in the nanoparticles, and the PLA/TPGS component ratio of the copolymer. *In vitro* cellular uptake of fluorescent-loaded PLA–TPGS nanoparticles by HT-29 cells exhibited dependency on the TPGS composition in the copolymer. *In vivo* investigations on rats demonstrated that the paclitaxel-loaded PLA–TPGS nanoparticles increased the blood circulation time of the drug up to 224.5 h in comparison of 22.9 h for Taxol® after i.v. administration of the same 10 mg/kg dose. Moreover, the nanoparticle formulation exhibited much higher therapeutic efficiency represented by much larger total AUC and much lower side effects represented by much smaller AUC located above the maximum tolerance compared with Taxol®. HT-29 xenograft tumor model on SCID mice showed that paclitaxel formulated in the PLA–TPGS nanoparticles can effectively inhibit the growth of tumor over a longer period of time than Taxol® at the same dose. It can thus be concluded that PLA–TPGS nanoparticle formulation could be much more effective than Taxol® in cancer treatment and cancer nanoparticle technology is feasible.

ACKNOWLEDGMENTS

The authors are grateful of Mr. Min Sung Chong, FYP students in Department of Chemical and Biomolecular Engineering, National University of Singapore, for their assistance in experiments and Dr. Linyun Zhao for the HPLC analysis method on plasma samples. This research was supported by A*STAR BMRC Singapore Cancer Syndicate Grant UU0028 (SS Feng, PI) and NUS FRC Grant R279-000-226-112 (SS Feng, PI). Zhang ZP thanks NUS for the financial support for his Ph.D. study and Lee SH thanks EDB and NUSNNI for the financial support for her M.Eng. study.

REFERENCES

1. R. C. Donehower, E. K. Rowinsky, L. B. Grochow, and S. M. Longnecker. Phase I trial of Taxol in patients with advanced cancer. *Cancer Treat. Rep* **71**:1171–1177 (1987).
2. N. M. Lopes, E. G. Adams, T. W. Pitts, and B. K. Bhuyan. Cell kill kinetics and cell-cycle effects of taxol on human and hamster ovarian cell lines. *Cancer Chemother. Pharmacol* **32**:235–242 (1993).
3. M. C. Wani, H. L. Taylor, and M. E. Wall. Plant antitumor agents VI. The isolation and structure of taxol, a novel antileukemic and antitumor agent from *Taxus brevifolia*. *J. Am. Chem. Soc* **93**:2325–2327 (1971).
4. R. T. Dorr. Pharmacology and toxicology of Cremophor EL diluent. *Ann. Pharmacother* **28**:S11–S14 (1994).
5. M. Kongshaug, L. S. Cheng, J. Moan, and C. Rimington. Interaction of Cremophor EL with human plasma. *Int. J. Biochem* **23**:473–478 (1991).
6. R. B. Weiss, R. C. Donehower, P. H. Wiernik, T. Ohnuma, R. J. Gralla, D. L. Trump, J. R. Baker, D. A. EchoVan, D. D. HoffVon, and B. Leyland Jones. Hypersensitivity reactions from taxol. *J. Clin. Oncol* **8**:1263–1268 (1990).
7. S. S. Feng and S. Chien. Chemotherapeutic engineering: Application and further development of chemical engineering principles for chemotherapy of cancer and other diseases. *Chem. Eng. Sci* **58**:4087–4114 (2003).

8. S. S. Feng. Nanoparticles of biodegradable polymers for new-concept chemotherapy. *Expert Rev. Med. Devices* **1**:115–125 (2004).
9. K. Fu, D. W. Pack, A. M. Klibanov, and R. Langer. Visual evidence of acidic environment within degrading poly(lactic-co-glycolic acid) (PLGA) microspheres. *Pharm. Res* **17**:100–106 (2000).
10. S. B. Zhou, X. Y. Liao, X. H. Li, X. M. Deng, and H. Li. Poly-D, L-lactide-co-poly(ethylene glycol) microspheres as potential vaccine delivery systems. *J. Control. Release* **86**:195–205 (2003).
11. W. J. Krasavage and C. J. Terhaar. D-alpha-tocopheryl poly (ethylene glycol) 1000 succinate—acute toxicity, subchronic feeding, reproduction, and teratologic studies in rat. *J. Agric. Food Chem* **25**:273–278 (1977).
12. K. Bogman, F. Erne-Brand, J. Alsenz, and J. Drewe. The role of surfactants in the reversal of active transport mediated by multidrug resistance proteins. *J. Pharm. Sci* **92**:1250–1261 (2003).
13. T. Chang, L. Z. Benet, and M. F. Hebert. The effect of water-soluble Vitamin-E (TPGS) on oral cyclosporine pharmacokinetics in healthy-volunteers. *Clin. Pharmacol. Ther* **57**:297–303 (1995).
14. Y. V. R. Prasad, S. P. Puthli, S. Eaimtrakarn, M. Ishida, Y. Yoshikawa, N. Shibata, and K. Takada. Enhanced intestinal absorption of vancomycin with Labrasol and D-a-tocopheryl PEG 1000 succinate in rats. *Int. J. Pharm* **250**:181–190 (2003).
15. L. Yu, A. Bridgers, J. Polli, A. Vickers, S. Long, A. Roy, R. Winnike, and M. Coffin. Vitamin E-TPGS increases absorption flux of an HIV protease inhibitor by enhancing its solubility and permeability. *Pharm. Res* **16**:1812–1817 (1999).
16. J. M. Dintaman and J. A. Silverman. Inhibition of P-glycoprotein by D-alpha-tocopheryl polyethylene glycol 1000 succinate (TPGS). *Pharm. Res* **16**:1550–1556 (1999).
17. J. R. Fischer, K. R. Harkin, and L. C. Freeman. Concurrent administration of water-soluble vitamin E can increase the oral bioavailability of cyclosporine A in healthy dogs. *Vet. Ther* **3**:465–473 (2002).
18. L. Mu and S. S. Feng. Vitamin E TPGS used as emulsifier in the solvent evaporation/extraction technique for fabrication of polymeric nanospheres for controlled release of paclitaxel (TaxolÒ). *J. Control. Release* **80**:129–144 (2002).
19. L. Mu and S. S. Feng. A novel controlled release formulation for the anticancer drug paclitaxel (TaxolÒ): PLGA nanoparticles containing vitamin E TPGS. *J. Control. Release* **86**:33–48 (2003).
20. K. Y. Win and S. S. Feng. Effects of particles size and surface coating on cellular uptake of polymeric nanoparticles for oral delivery of anticancer drugs. *Biomaterials* **26**:2713–2722 (2005).
21. K. Y. Win and S. S. Feng. *In vitro* and *in vivo* studies on vitamin E TPGS-emulsified poly(D, L-lactic-*co*-glycolic acid) nanoparticles for paclitaxel formulation. *Biomaterials* **27**:2285–2291 (2006).
22. Z. Zhang and S. S. Feng. Nanoparticles of poly(lactide)/vitamin E TPGS copolymer for cancer chemotherapy: Synthesis, formulation, characterization and *in vitro* drug release. *Biomaterials* **27**:262–270 (2006).
23. Z. Zhang and S. S. Feng. The drug encapsulation efficiency, *in vitro* drug release, cellular uptake and cytotoxicity of paclitaxel-loaded poly(lactide)-tocopheryl polyethylene glycol succinate nanoparticles. *Biomaterials* **27**:4025–4033 (2006).
24. Z. Zhang and S. S. Feng. Self-assembled nanoparticles of poly (lactide)-Vitamin E TPGS copolymers for oral chemotherapy. *Int. J. Pharm* **324**:191–198 (2006).
25. J. Ryu, Y. I. Jeong, I. S. Kim, J. H. Lee, J. W. Nah, and S. H. Kim. Clonazepam release from core-shell type nanoparticles of poly(epsilon-caprolactone)/poly(ethylene glycol)/poly(epsilon-caprolactone) triblock copolymers. *Int. J. Pharm* **200**:231–242 (2002).
26. L. W. Seymour. Passive tumor targeting of soluble macromolecules and drug conjugates. *Crit. Rev. Ther. Drug Carrier Syst* **9**:135–187 (1992).
27. H. Maeda, J. Wu, T. Sawa, Y. Matsumura, and K. Hori. Tumor vascular permeability and the EPR effect in macromolecular therapeutics: a review. *J. Control. Release* **65**:271–284 (2000).
28. Y. Dong and S. S. Feng. Methoxy poly(ethylene glycol)-poly (lactide) (MPEG-PLA) nanoparticles for controlled delivery of anticancer drugs. *Biomaterials* **25**:2843–2849 (2004).
29. T. Govender, S. Stolnik, M. C. Garnett, L. Illum, and S. S. Davis. PLGA nanoparticles prepared by nanoprecipitation: drug loading and release studies of a water soluble drug. *J. Control. Release* **57**:171–185 (1999).
30. W. J. Lin, L. W. Juang, and C. C. Lin. Stability and release performance of a series of pegylated copolymeric micelles. *Pharm. Res* **20**:668–73 (2003).
31. J. E. Liebmann, J. A. Cook, C. Lipschultz, D. Teague, J. Fisher, and J. B. Mitchell. Cytotoxic studies of paclitaxel (Taxol) in human tumor cell lines. *Br. J. Cancer* **68**:1104–1109 (1993).
32. E. S. Lee, K. Na, and Y. H. Bae. Doxorubicin loaded pH-sensitive polymeric micelles for reversal of resistant MCF-7 tumor. *J. Control. Release* **103**:405–418 (2005).
33. Z. Xu, W. Gu, J. Huang, H. Sui, Z. Zhou, Y. Yang, Z. Yan, and Y. Li. *In vitro* and *in vivo* evaluation of actively targetable nanoparticles for paclitaxel delivery. *Int. J. Pharm* **288**:361–368 (2005).
34. Y. Chen, G. Dalwadi, and H. A. E. Benson. Drug delivery across the blood–brain barrier. *Curr. Drug Deliv* **1**:361–76 (2004).
35. A. Moreno, L. A. Lopez, A. Fabra, and C. Arus. ^{1}H MRS markers of tumor growth in intrasplenic tumors and liver metastasis induced by injection of HT-29 cells in nude mice spleen. *NMR Biomed* **11**:93–106 (1998).
36. M. G. Sacco, S. Soldati, E. Mira Cato, L. Cattaneo, G. Pratesi, E. Scanziani, and P. Vezzoni. Combined effects on tumor growth and metastasis by anti-estrogenic and antiangiogenic therapies in MMTV-neu mice. *Gene Ther* **9**:1338–1341 (2002).